Interactions of Molecular Hydrogen with Alkali Metal Halides in Argon Matrices: A Computational Model

Michael L. McKee*,[1] and Ray L. Sweany*,[2]

Departments of Chemistry, Auburn University, Auburn, Alabama 36849, and University of New Orleans, New Orleans, Louisana 70148-2820

Received: June 29, 1999; In Final Form: November 17, 1999

MP2 calculations have been performed in order to understand the behavior of molecular hydrogen in gas matrices containing alkali metal halide ion pairs. Calculations that model interactions between H_2 and LiCl, NaCl, KCl, KF, and NaF were augmented by the addition of argon atoms. Interactions between CuCl and dihydrogen were also modeled for comparison purposes. The conformational space of H_2 with NaCl was explored extensively with and without Ar atoms. The frequency of the H−H stretch is sensitive to the orientation and position of H_2 relative to NaCl, with frequency shifts spanning nearly 60 cm^{-1}. Zero-point corrections were scaled differently depending on the nature of the vibrational modes. For modes that are characterized by deep potentials, a scaling factor of 0.93 was used. For the low-energy vibrations that result from the associations of two weakly bound particles, a scaling factor of only 0.26 was used to compensate for the inappropriateness of a harmonic oscillator approximation. KF binds H_2 most strongly at the fluoride ion, while NaF, KCl, NaCl, and LiCl involve increasing participation by the cation in the binding. The binding energies range from 1.5 to 2.1 kcal/mol. Except for KF and LiCl, the hydrogen interacts with both the anion and cation in varying degrees. Except in LiCl, argon competes successfully with H_2 for binding at the cation site and hydrogen is displaced totally from the cation site by argon atoms, as demonstrated by calculations of $[NaAr_x(H_2)]Cl$ for $x = 1-5$.

Introduction

The H−H stretching vibration of molecular hydrogen becomes observable by infrared spectroscopy because of perturbations caused by the environment. In particular, in rare gas matrices doped with alkali metal halides, the intensity of the H−H stretching vibration becomes the strongest feature in the spectrum of the aggregate, the position being red-shifted from 40 to 120 cm^{-1}.[3,4] Similar perturbations have been noted in zeolites and on surfaces of alkali metal halides.[5,6] By contrast, it is often difficult to observe dihydrogen that has coordinated to the metal of organometallic complexes, yet the red-shifts of the H−H stretching vibrations are on the order of 1000 cm^{-1}.[7,8] The matrix studies of alkali metal halides in argon allowed a great deal of variation in the sizes of the cations and anions in contact with hydrogen.[3,4] Anions have the largest influence on the position of the H−H stretch, whereas there is virtually no evidence of a cation influence.[3] In contrast with the perturbations induced by the anions of the alkali metal halides, CuCl causes an extreme red-shift of the H−H stretching vibration, which is attributed to an interaction with Cu(I).[9] If Cu(I) can be considered a pseudo alkali metal, then this observation is particularly hard to explain. Of the alkali metal chlorides, only with NaCl are there features suggesting that the sodium ion is influencing the spectrum. In the H−H stretching region, NaCl causes multiple absorptions that became simplified upon annealing.[4] The different absorptions probably arise from hydrogen in different environments, but it seemed unlikely that argon could be the differentiating factor. Rather, the multiple absorptions are probably due to conformers that involve differing degrees of interaction between H_2, the cation, and the anion. In this model, the role of the argon may only be to contribute to the barrier to transformations between the conformers.

The matrix experiments were not able to differentiate between explanations of why the cation of most alkali metal halides did not affect the spectrum. Either argon preferentially solvated the cation sites of the alkali metal halides or the cation could not produce a great deal of intensity because of the symmetry of the aggregate. Analogies drawn from H_3^+ leads to an expectation of a T-shape as H_2 interacts with the cation of an ion pair, similar to the geometry of organometallic dihydrogen complexes.[10] Since Raman spectroscopy of matrices did not produce evidence of hydrogen of any sort in dilute matrices,[11] it appears that the issue may only be settled by computational modeling. We have undertaken to address two issues in our work. Does the presence of Ar prevent access of hydrogen to cation sites in matrix experiments? Do the explanations seem plausible that were offered to explain the unusual appearance of the spectrum in the H−H stretching region in Ar matrices of NaCl? Finally, why is the behavior of H_2−CuCl so different from what is exhibited by H_2−MX?[9]

Computational Methods

All geometries were fully optimized in the given symmetry at the MP2(FULL)/6-311++G(d) level with the OPT=TIGHT option.[12,13] Vibrational frequencies were calculated at that level (except for larger $[NaAr_n(H_2)]Cl$ complexes) to determine the nature of the stationary points. Single-point calculations at the MP2(FULL)/6-311++G(3df,2p) level on MP2(FULL)/6-311++G(d) geometries with zero-point correction at the MP2-(FULL)/6-311++G(d) will constitute the "standard" level. The interparticle, vibrational potential for van der Waals adducts is not well-modeled by a harmonic potential.[14−16] The results of our calculations overestimate the vibrational frequencies and, hence, the zero point correction. Therefore, we have used two difference scaling factors for computing zero-point corrections.

10.1021/jp992207o CCC: $19.00
Published on Web 01/14/2000

We have used a 0.93 scaling factor for the H−H and M−X stretches,[17] and a 0.26 factor for interfragment vibrations. The former is the average of scaling factors determined for HF/TZ2P and CISD/TZ2P methods. We determined the latter value by comparing results for the linear complex, CN−H_2, with frequencies fit to a high-level potential energy surface.[18] The ratio between our interfragment zero-point energy and the fitted value was 0.21. Also, we found that the interfragment, zero-point energy was very different for the Ar−H_2 complex in the side-on and end-on orientation. Without a substantial reduction in these zero-point energies, end-on binding is predicted to be unfavorable. A 0.26 scaling leads to the same binding in both orientations. Clearly, uncertainties in the zero-point correction will lead to uncertainties in the relative energies of adducts. The proposed remedy will reduce the error but treats all potentials of van der Waals modes equivalently, a point that lacks justification. However, it is probably unnecessary to tweak the correction further. The argon cage will contribute to the potential for these large amplitude vibrations, making a realistic representation beyond reach.

Basis set superposition error (BSSE) corrections have not been made and could reduce the calculated binding energy. Nevertheless, the level of theory that we have used is able to model several systems for which there is either experimental underpinning or more advanced calculations on identical systems. The calculated binding energy of Ar_2 is 0.27 kcal/mol (94 cm^{-1}), while the experiment gives 85 cm^{-1}.[19] The calculated binding energy of $ArNa^+$ (4.22 kcal/mol; 1476 cm^{-1}) is in good agreement with an accurate theoretical value of 1330 cm^{-1}.[20] Ar−NaCl has been examined by microwave techniques. It is linear on average with a binding energy determined to be 1.9 kcal/mol, as obtained by a coupled-cluster calculation, in good agreement with our own 2.0 kcal/mol.[21] An analysis of the microwave data showed that charge transfer between argon and the sodium ion could not be ignored. We have shown a substantial amount of charge transfer in our computed results. Finally, a recent experimental determination of binding in the Ar−Cl^- complex gives a value of 1.50 kcal/mol that can be compared to our computed value of 1.21 kcal/mol.[22]

The calculations involving copper (CuCl, Ar−CuCl, H_2−CuCl) used the 10 electron Stuttgard/Dresden ECP with the valence electrons described with a (8s,7p,6d) basis set contracted to (6s,5p,3d) and a 6-311++G(d) basis set for chlorine and hydrogen.

Results and Interpretation

An analysis of interactions of alkali metal halides in rare gas matrices began by modeling MX interactions with H_2 in the vacuum. Next, we undertook a study of the interaction of MX with Ar. Finally, we undertook a study that examined the interaction of NaCl with dihydrogen in the presence of up to five atoms of argon.

H_2−MX in a Vacuum. To gauge the accuracy of our approach, the T-shaped aggregate H_2−NaCl was treated by the standard MP2 approach and also by the QCISD method. These results are found in Table 1. There is good agreement for most features of the vibrational spectrum. Neither model is capable of reproducing experimental values of the H−H stretch, hence the need for scaling. The difference between the perturbed and unperturbed position can still be meaningful. For KF−H_2 (IV), the difference is estimated to be 121 cm^{-1} using the MP2 method. Experimentally, the difference is 130 cm^{-1}.[4] For KCl−H_2, the difference is 42 cm^{-1} at the same level of theory. The observed difference is 65 cm^{-1}.[3] Thus, the method is capable of achieving differences that are within the range of experimental differences.

TABLE 1: Comparison of Vibrational Frequencies (cm^{-1}) and Intensities (km/mol) for H_2, NaCl and the Side-on H_2-NaCl Complex, C_{2v}

	symmetry	MP2(full)[a]	QCISD(full)[a]
H_2		4458(0.0)[b,c]	4266(0.0)[b,c]
NaCl		370(57.0)[d]	370(56.2)[d]
H_2−NaCl	a_1	4419(13.5)	4234(10.8)
	b_2	452(5.6)	436(5.1)
	a_1	376(63.8)	375(63.0)
	a_1	233(0.0)	226(0.1)
	b_1	47(9.7)	47(9.7)
	b_2	36(8.9)	36(9.0)

[a] Basis set a is 6-311++G(d). [b] Intensities are given in parentheses. [c] Gas-phase Raman position at 4161 cm^{-1},[23] matrix position at 4144 cm^{-1}.[3] [d] Matrix position 335 cm^{-1}.[3]

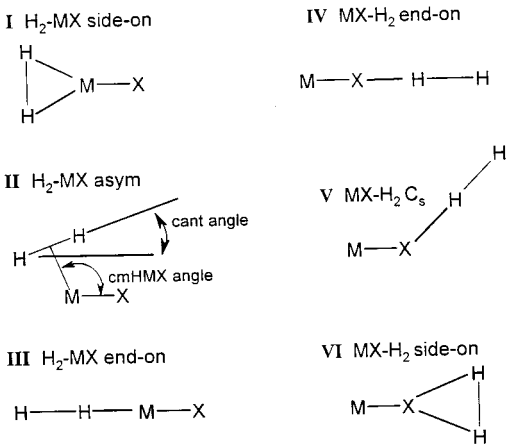

Figure 1. Structures of conformers of H_2:MX.

The energies for the reactions of H_2 and MX have been calculated using MP2 methods with two basis sets. The results are summarized in Tables 2 and 3. Because NaCl behaves uniquely in the matrix, it was desirable to explore the energy of this interaction in the greatest detail. The geometry was constrained in various fashions in order to map out the energy as a function of the orientation and position of the dihydrogen. The various geometries are illustrated in Figure 1. The global minimum in the electronic energy was found to be for an isomer of C_s symmetry with H_2 simultaneously interacting with sodium and, to a lessor extent, with the chloride (II). The angle cmHNaCl, where cmH is the center of mass of the H_2, is 110° and the hydrogen is canted away from the chloride by 16°. We presume an electrostatic interaction with the chloride although the nearest hydrogen is 3.83 Å away from the chloride because there is no maximum in the electrostatic potential off the NaCl axis.[24] The T-shaped isomer of C_{2v} symmetry (I) is less favored both electronically and when the zero-point correction is applied. The T-shaped molecule resembles the most stable form of H_2−LiCl and H_2−CuCl that has been observed in matrices and for which MP2 calculations have also been performed.[9] Still less stable by 1.8 kcal/mol is the aggregate of $C_{\infty v}$ symmetry in which dihydrogen approaches the sodium end-on (III). Finally, an end-on arrangement (IV) of dihydrogen in proximity of the chloride ion was nearly half as tightly bound as it was on the sodium side.

The frequency shift of the H−H stretch for the various isomers of NaCl−H_2 ranged over 58 cm^{-1}. The highest frequency was calculated for the isomer with hydrogen bonded end-on to the sodium ion (III). In fact, the position of the H−H stretch was found to be above that of unperturbed dihydrogen. The ionic potential of the sodium ion polarizes the H−H bond, resulting in a stronger and shorter H−H bond, and hence a

TABLE 2: Absolute Energies (Hartrees), Zero-Point Energies (kcal/mol), and Vibrational Frequencies

						ω (cm^{-1})[f]	
	shape[a]	MP2(full)[b]	ZPE[c] intrafrag	ZPE[d] intrafrag	MP2(full)[e]	MX	H_2
H_2	$D_{\infty h}$	−1.14591	5.92(0)		−1.16280		4146
Ar	K	−527.00829	0		−527.11026		
Ar_2	$D_{\infty h}$	−1054.01684		0.01(0)	−1054.22096		
Ar−H_2 side-on	C_{2v}	−528.15423	5.93(1)	0.01	−528.27314		4144
Ar−H_2 end-on	$C_{\infty v}$	−528.15438	5.92(0)	0.13	−528.27333		4144
Na^+	K	−161.79381	0		−161.8127		
Cl^-	K	−459.75277	0		−459.85951		
Na^+−Ar	$C_{\infty v}$	−688.80764		0.05(0)	−688.92977		
Cl^-−Ar	$C_{\infty v}$	−986.76196		0.01(0)	−986.97172		
NaCl	$C_{\infty v}$	−621.75757	0.49(0)		−621.88334	344	
Ar−NaCl	$C_{\infty v}$	−1148.76887	0.50(0)	0.05	−1148.99677	349	
Ar−NaCl bent	C_s	−1148.76883	0.50(0)	0.04	−1148.99676	349	
NaCl−Ar	$C_{\infty v}$	−1148.76661	0.49(0)	0.02	−1148.99475	345	
H_2−NaCl side-on	C_{2v}/I	−622.90567	6.36(0)	0.26	−623.04902	350	4102
H_2−NaCl asym	C_s/II	−622.90548	6.35(0)	0.30	−623.04922	342	4102
H_2−NaCl end-on	$C_{\infty v}$/III	−622.90382	6.43(0)	0.20	−623.04608	345	4152
[NaAr(H_2)]Cl	C_s/A1	−1149.91671	6.35(0)	0.43	−1150.16289	345	4094
[$NaAr_2$(H_2)]Cl	C_1/A2	−1676.92776	6.35(0)	0.48		343	4098
[$NaAr_3$(H_2)]Cl	C_s/A3	−2203.93893					
[$NaAr_4$(H_2)]Cl	C_s/A4	−2730.95034					
[$NaAr_5$]Cl	C_{4v}/A6	−3256.81374					
[$NaAr_5$][Cl(H_2)]	C_s/A5	−3257.96141					
NaCl−H_2 end-on	$C_{\infty v}$/IV	−622.90470	6.38(0)	0.32	−623.04780	344	4117
[NaAr][ClH_2]	$C_{\infty v}$	−1149.91610	6.38(0)	0.41	−1150.16124	349	4116
NaCl−H_2 side-on	C_{2v}/VI	−622.90352	6.42(1)	0.02	−623.04625	345	4146
KCl	$C_{\infty v}$	−1059.20251	0.36(0)		−1059.38908	256	
Ar−KCl	C_s	−1586.21190	0.36(1)	0.01	−1586.50101	255	
KCl−Ar	$C_{\infty v}$	−1586.21146	0.36(0)	0.01	−1586.50041	255	
H_2−KCl side-on	C_{2v}/I	−1060.34912	6.27(1)	0.11	−1060.55311	255	4130
H_2−KCl asym	C_s/II	−1060.35010	6.21(0)	0.32	−1060.55469	254	4091
KCl−H_2 end-on	$C_{\infty v}$/IV	−1060.34978	6.23(2)	0.43	−1060.55376	254	4107
KCl−H_2 side-on	C_{2v}/VI	−1060.34842	6.29(1)	0.01	−1060.55193	255	4144
^{7}LiCl	$C_{\infty v}$	−467.25142	0.88(0)		−467.35330	618	
Ar−^{7}LiCl	$C_{\infty v}$	−994.26602	0.92(0)	0.36	−994.46818	641	
H_2−^{7}LiCl	C_{2v}/I	−468.40226	6.76(0)	0.44	−468.52095	645	4082
CuCl	$C_{\infty v}$	−656.31661	0.56(0)		−656.41813	392	
Ar−CuCl	$C_{\infty v}$	−1183.33694	0.59(0)	0.09	−1183.54069	413	
H_2−CuCl side-on	C_{2v}/I	−657.48994	5.38(0)	0.75	−657.61717	409	3357
NaF	$C_{\infty v}$	−261.73303	0.68(0)		−261.81438	476	
H_2−NaF side-on	C_{2v}/I	−262.88090	6.56(0)	0.29	−262.97969	477	4112
H_2−NaF asym	C_s/II	−262.88108	6.47(0)	0.44	−262.98101	471	4057
NaF−H_2 end-on	$C_{\infty v}$/IV	−262.88126	6.46(0)	0.46	−262.98028	476	4046
KF	$C_{\infty v}$	−699.18134	0.55(0)		−699.3204	385	
Ar−KF	$C_{\infty v}$	−1226.19045	0.55(1)	0.01	−1226.43201	384	
KF−Ar	$C_{\infty v}$	−1226.19039	0.55(0)	0.02	−1226.43202	386	
KF−H_2 end-on	$C_{\infty v}$/IV	−700.32972	6.44(2)	0.22	−700.48661	384	4033
KF−H_2 bent	C_s/V	−700.32979	6.31(0)	0.43	−700.48657	383	4034

[a] Roman numerals and A*x* refer to labels in Figures 1 and 2, respectively. [b] Basis set is 6-311++G(d). [c] Modes that are well-approximated by a harmonic potential, scaled by 0.93, calculated using basis set a, MP2(full)/6-311++G(d). Number in parentheses is the number of imaginary vibrational frequencies. [d] Modes that are poorly approximated by a harmonic potential, scaled by 0.26, calculated using basis set a, MP2(full)/6-311++G(d). Number in parentheses is the number of imaginary vibrational frequencies. [e] Basis set is 6-311++G(3df,2p) [f] Calculated using the 6-311++G(d) basis set, scaled by 0.93

higher stretching frequency; there is a shift of 0.15 electrons within the dihydrogen molecule. The more stable side-on bonded hydrogen (I) is characterized by a red-shift in the H−H stretching vibration of 44 cm^{-1}. The shift is similar to what is calculated for IV (27 cm^{-1}), where H_2 binds end-on to the chloride. The similarity in position of these two absorptions makes it unlikely that the site of coordination can be firmly established by the position of the H−H stretching vibration. Indeed, absorptions in the same region of the spectrum have already been assigned to hydrogen associated with cation and anion sites.[2−6] This work suggests that the assignments are mutually compatible.

It is interesting to speculate on the consequences if hydrogen rotates in its position next to a sodium ion or chloride ion. Taking the former, the hydrogen will explore environments that will result in its infrared absorption ranging over 50 cm^{-1}. Significant broadening will appear in the spectrum if the hydrogen rotates at or near its free rotor rate in a fashion so that it becomes alternately end-on and side-on. Rotation of hydrogen at the chloride side results in a 29 cm^{-1} range of frequencies. One can estimate barriers to rotation from the structures that we have sampled. For rotations about an axis that is perpendicular to the NaCl bond vector, the barrier heights are at least 1.85 and 0.65 kcal/mol for hydrogen linked via sodium and chloride, respectively. The barrier to rotations about an axis parallel to the NaCl bond vector is presumably zero except as the argon cage restricts the rotation. Hence, ortho and para forms should be distinguishable for the isomers of C_{2v} symmetry. No attempt was made to compute a barrier for rotation for the isomer of C_s symmetry (II).

The intensity of the H−H stretch of the side-on bonded H_2−NaCl is surprisingly high (11 km/mol) and results from the

TABLE 3: Reaction Energies (kcal/mol) for Formation of Complexes at MP2 Optimized Geometries

	shape[a]	MP2(full)[b]	MP2(full)[c]	+MZPC[d]
Ar_2	$D_{\infty h}$	−0.16	−0.28	−0.27
Ar−H_2 side-on	C_{2v}	−0.02	−0.05	−0.04
Ar−H_2 end-on	$C_{\infty v}$	−0.11	−0.17	−0.04
Na^+−Ar	$C_{\infty v}$	−3.48	−4.27	−4.22
Cl^-−Ar	$C_{\infty v}$	−0.56	−1.22	−1.21
Ar−NaCl	$C_{\infty v}$	−1.89	−1.99	−1.93
Ar−NaCl bent	C_s	−1.86	−1.98	−2.04
NaCl−Ar	$C_{\infty v}$	−0.47	−0.72	−0.70
H_2−NaCl side-on	C_{2v}/I	−1.37	−1.81	−1.60
H_2−NaCl asym	C_s/II	−1.22	−1.93	−1.73
H_2−NaCl end-on	$C_{\infty v}$/III	−0.21	0.04	0.25
[NaAr(H_2)]Cl	C_s/A1	−3.10	−4.07	−3.68
[$NaAr_2$(H_2)]Cl	C_1/A2	−4.83		
[$NaAr_3$(H_2)]Cl	C_s/A3	−6.64		
[$NaAr_4$(H_2)]Cl	C_s/A4	−8.60		
[$NaAr_5$]Cl	C_{4v}/A6	−9.24		
[$NaAr_5$][Cl(H_2)]	C_s/A5	−9.72		
NaCl−H_2 end-on	$C_{\infty v}$/IV	−0.76	−1.04	−0.75
[NaAr][ClH_2]	$C_{\infty v}$	−2.72	−3.04	−2.67
NaCl−H_2 side-on	C_{2v}/VI	−0.02	−0.07	−0.10
Ar−KCl	C_s	−0.69	−1.05	−1.03
KCl−Ar	$C_{\infty v}$	−0.41	−0.67	−0.66
H_2−KCl side-on	C_{2v}/I	−0.44	−0.77	−0.67
H_2−KCl asym	C_s/II	−1.05	−1.76	−1.52
KCl−H_2 end-on	$C_{\infty v}$/IV	−0.85	−1.18	−0.53
KCl−H_2 side-on	C_{2v}/VI	0.00	−0.03	−0.01
Ar−LiCl	$C_{\infty v}$	−3.96	−2.90	−2.50
H_2−LiCl	C_{2v}/I	−3.09	−3.04	−2.64
Ar−CuCl	$C_{\infty v}$	−7.56	−7.72	−7.61
H_2−CuCl side-on	C_{2v}/I	−17.21	−22.74	−23.09
H_2−NaF side-on	C_{2v}/I	−1.23	−1.58	−1.33
H_2−NaF asym	C_s/II	−1.34	−2.40	−2.10
NaF−H_2 end-on	$C_{\infty v}$/IV	−1.46	−1.94	−1.60
Ar−KF	$C_{\infty v}$	−0.51	−0.85	−0.84
KF−Ar	$C_{\infty v}$	−0.48	−0.85	−0.83
KF−H_2 end-on	$C_{\infty v}$/IV	−1.55	−2.14	−1.94
KF−H_2 bent	C_s/V	−1.59	−2.11	−1.85

[a] Roman numerals and A*x* refers to designations in Figures 1 and 2, respectively. [b] Calculated with the 6-311++G(d) basis set. [c] Calculated with the 6-311++G(3df,2p) basis set. [d] Modified zero-point correction applied to relative energies in the previous column. The H_2 and MX stretches are scaled by 0.93, while the interfragment frequencies are scaled by 0.26.

electrons of the molecule oscillating in the direction of the sodium ion as the H−H bond is extended. The perpendicular polarizability derivative for the H−H stretch has been calculated to be about half that of the parallel polarizability derivative.[25] The fact that hydrogen is so difficult to observe in transition metal complexes of hydrogen must be ascribed to the absence of a large ionic charge on the metal. The charge on the sodium ion can be inferred from the dipole moment and is +0.79, or from our model, 0.63.[26] The implication is that the charge of the metal in organometallic complexes must be less than 0.7 for the H−H stretch to be so difficult to observe, which is reasonable given the low oxidation state of the metal and the presence of good donor atoms in the coordination sphere. For NaCl, the intensity of the H−H stretch is largest for the end-on orientations at either side of the ion-pair (19 and 24 km/mol).

Less detailed calculations were performed for the other alkali metal halides. With LiCl, the T-shaped isomer (I) is most stable. For H_2−KCl, the asymmetric isomer (II) is most stable but it differs from that of H_2−NaCl. The chloride plays a much more significant role in the KCl adduct. The cmHKCl angle is now only 60°, and the H_2 is canted toward the chloride by 35°. The separation of the nearest hydrogen to chloride is shortened to 3.15 Å compared to the 3.83 Å approach in the analogous isomer of H_2−NaCl. This increased importance of the chloride also is reflected in the fact that chloride coordination (IV) is nearly as favored as the T-shaped isomer (I). Experimentally, KCl−H_2 gives a single absorption at 4079 cm^{-1},[3] at somewhat lower energy to that calculated for any of the isomers. To summarize, the trend seen in our calculations has the H_2 in the process of being passed from the cation (LiCl) to the anion in H_2−KCl as the cation swells. Presumably, the transfer would be complete in adducts of RbCl and CsCl.

By contrast to NaCl, KF binds hydrogen through its fluoride ion (V) and the potassium ion is remote to the hydrogen. The cmHKF angle is only 17°. The H−H bond is almost directly pointed at the fluorine, deviating by only 3°. This is a result of a combination of factors, principally the larger size of the potassium ion and the smaller size of the fluoride. In NaF−H_2, for example, the orientation of the H_2 is nearly identical to KCl−H_2 (II). In H_2−NaF, the cmHNaF angle is 60°. Although the H_2 is still pointed at the fluoride, the angle deviates by 38° from linearity, canted toward the sodium. Simons has undertaken extensive calculations on H_2F^- and has found the pair are bound by 4.7 kcal/mol even after the zero-point contribution is added to the electronic energy.[27] For KF−H_2, the pair is only bound by 1.94 kcal/mol. The smaller charge on fluorine may account for some of the difference. The frequency for the H−H stretch is found experimentally at 4014 cm^{-1}, 20 cm^{-1} to the red of what was calculated. The calculated intensity of the H−H stretch (8 km/mol) is nearly as great as the K−F stretch, in accord with experiment.

Since the d orbitals of Cu(I) have become quite stable, they may be viewed in some sense as core orbitals. Hence, it is interesting to think of CuCl as a pseudo alkali metal halide. The interactions between H_2 and CuCl have been explored experimentally and by similar MP2 methods as we have used in our studies.[9] Our computational results agree with what has been already reported. By contrast to the alkali metals, there is significant covalent bonding between CuCl and H_2 (I) involving the 4s/4p orbitals that results in significant charge transfer of 0.28 electrons. The position of the H−H stretch is accordingly found at a very much lower frequency, shifted by 845 cm^{-1} from the position of unperturbed hydrogen. Even with the much more acidic BeO, the position of the H−H stretch is only expected to shift by 569 cm^{-1}.[28]

When the zero-point energy correction is added to the electronic energy, the system becomes less bound relative to the separated particles for all systems studied. The zero-point correction has two origins. First, the two normal modes of the aggregate that correlate to normal modes in the separated particles will contribute to the stability of the aggregate to the extent that the frequencies red-shift upon coordination. Second, depending on the structure, four new modes in the aggregate are created out of rotational and translational modes of the separated particles. These modes have already been described (vide supra) and will always result in a cancelation of at least some of energy advantage of dipole−induced dipole interactions. However, because of the slow relaxation of *o*-H_2, 0.50 kcal/mol of rotational energy remains with the separated particles even at low temperatures. For *o*-H_2, this "zero-point" rotational energy will subtract 0.5 kcal/mol from those energies tabulated in Table 3, a significant contribution toward the stabilization of the adducts of *o*-H_2.

Ar−MX. Argon prefers interacting with the cation of the MX ion pair. (See Tables 2 and 3.) The electronic energy favors a linear arrangement. As might be expected for an electrostatic interaction, the potential energy is quite flat for small variations in the angle. For Ar−NaCl the zero-point correction results in

TABLE 4: Calculated Reaction Energies (kcal/mol) for $[NaAr_y(H_2)_x]Cl$ ($x = 0, 1$; $y = 0-5$)

				contribution	
	shape[a]	MP2[b]	+MZPC[c]	per Ar	per H_2
[NaAr]Cl		−1.89	−1.83	−1.83	
$[NaAr_5]Cl$	A6	−9.24	−8.94	−1.78	
$[Na(H_2)]Cl$		−1.37	−1.16		−1.16
$[NaAr(H_2)]Cl$	A1	−3.10	−2.71	−1.81[d]	−0.90[d]
$[NaAr_2(H_2)]Cl$	A2	−4.83	−4.39	−1.81[d]	−0.77[d]
$[NaAr_3(H_2)]Cl$	A3	−6.64	−6.15	−1.81[d]	−0.72[d]
$[NaAr_4(H_2)]Cl$	A4	−8.60	−8.06	−1.81[d]	−0.82[d]
$[NaAr_5][Cl(H_2)]$	A5	−10.34	−9.72	−1.78[e]	−0.78[e]

[a] See Figure 2 for structures. [b] Basis set a is 6-311++G(d). [c] Modified zero-point correction applied to relative energies. The H_2 and MX stretches are scaled by 0.93, while the interfragment frequencies are scaled by 0.26. [d] Since the binding energy of argon is nearly constant from $x = 1$ and 5 for $y = 0$, a prorata argon binding energy of −1.81 kcal/mol is assumed. [e] Argon is assumed to bind to $[NaAr_5][Cl(H_2)]$ with a binding energy of 1.78 kcal/mol, the same as in $[NaAr_5]Cl$.

the argon atom moving off-axis to 170°. The angle shrinks to 164° in the KCl complex. Neither NaCl nor NaF appear to have any irregularities in the electrostatic potential that might lead them to interact electrostatically with a preferred orientation that is off-axis.[24] The argon is less strongly bound by a factor of 3 to the chloride ion in NaCl−Ar, the result of repulsions between the negative charge of chlorine and the electron density of the argon. The structure of the adduct has now been found to be linear experimentally, on average, with argon assoicated with the sodium ion.[21]

The electronic binding energy of the Ar−NaCl complex is 0.06 kcal/mol more negative than any H_2−NaCl conformer relative to the separated particles. The zero-point correction raises this advantage for Ar coordination to 0.31 kcal/mol. Argon is more favored over hydrogen on the cation site of KCl than is the case with NaCl. These preferences can be understood on the basis of an analysis of polarizability. Although the polarizability of argon is greater than for H_2,[29,30] this advantage is diminished because of the larger size of Ar. Although the perpendicular polarizability of hydrogen is less than the parallel polarizability, hydrogen still favors the perpendicular orientation because it can approach closer than it can in the parallel orientation. With the larger potassium, the small size of hydrogen is of less advantage.

The zero-point correction will always favor argon coordination. This is because argon has no rotational degrees of freedom. On the other hand, several vibrational modes of H_2−MX correlate with rotational as well as translational modes of the separated particles. Even at temperatures close to 0 K, these energies contribute to the energy of the adduct whereas the energy of translational and rotational modes of the separated particles can ordinarily be cooled to zero. *o*-H_2 is unique in retaining rotational energy even at 0 K. Thus, there is a zero-point rotational correction for ortho hydrogen of the separated particles that cancels some of the zero-point vibrational energy contribution in the adduct. Thus, *o*-H_2 should be more strongly bound than *p*-H_2.

$[NaAr_y(H_2)_x]Cl$. Having established that argon is more strongly bound than hydrogen to the sodium of NaCl, we then asked whether Ar would displace a hydrogen molecule that was already bound to the sodium ion. Ar atoms were added sequentially until a total of four were bound and hydrogen also remains bound to the cation. The results are summarized in Table 4 and illustrated in Figure 2. The additional argon atoms do not seriously change the Ar−NaCl binding energy, as demonstrated by comparisons of [NaAr]Cl and $[NaAr_5]Cl$. The

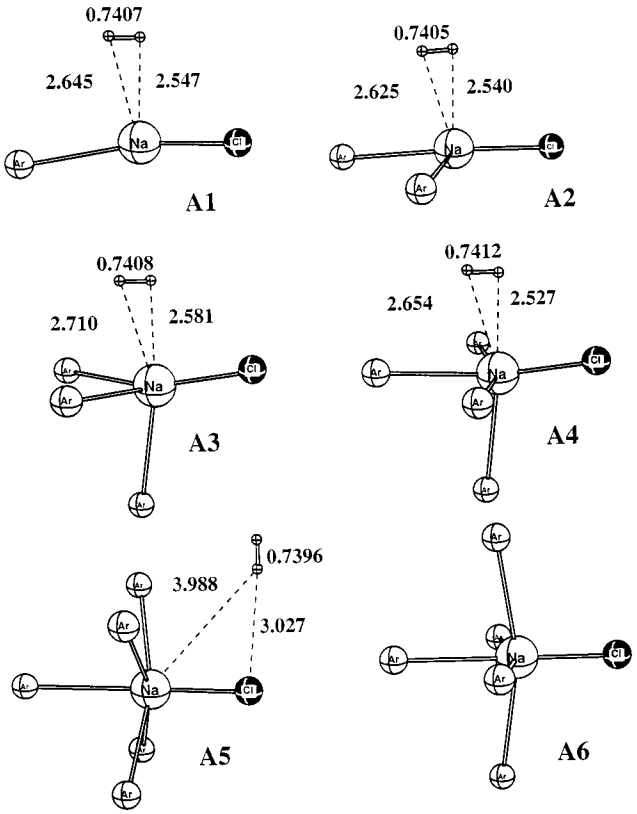

Figure 2. Structures of various confomers of $[NaAr_y(H_2)_x]Cl$.

additional argon atoms reduce the binding energy between the sodium ion and H_2 until binding at sodium or chloride has the same energetic consequence. With the addition of five argon atoms, the hydrogen molecule is displaced to the chloride side. Further coordination by argon at sodium is unlikely. In $[NaAr_5]$-$[Cl(H_2)]$, the hydrogen does not become trans to the sodium ion, however. The cmHClNa angle opens only to 101°. The hydrogen points at the chloride ion with a deviation of 9° from linearity. The distance of the center of mass of hydrogen from the sodium ion is 4.8 Å compared to 2.5 Å in I. Although this distance is large, the position of the H_2 suggests that there is some interaction. Moreover, the adjacent argon atoms are spread out to accommodate the hydrogen.

It is proper to ask whether argon might displace H_2 from the copper side of CuCl. We find that the binding of H_2 is much stronger to copper than argon. Hence, H_2 will probably not be displaced by argon. If H_2 did approach the chlorine of CuCl, it would experience a smaller charge (−0.33) on chlorine than it experiences for either KCl (−0.81) or NaCl (−0.63). The feature observed at 4122 cm^{-1} in argon matrices may be assignable to $CuCl-H_2$, which is far to the blue of the corresponding features for the alkali metal halides at 4075 cm^{-1}.[23]

In the matrix experiments, the absence of any significant change in the position of the H−H stretch as a function of the cation was used to defend the assertion that the anions were the cause of the perturbation that resulted in infrared intensity.[3] For the alkali metal chlorides, the position of the H−H stretch was nearly the same, varying by no more than 5 cm^{-1} from the average of 4080 cm^{-1}. On the other hand, the shift is 65 cm^{-1} on going from KCl to KF.[3,4] Does theory support the claim of anion binding of hydrogen? There are three scenarios that we have addressed by theory: cation binding, anion binding, and the asymmetric association. Clearly, cation binding of H_2 cannot occur and yield the experimental results. The calculated positions for the H−H stretch shifts by 30 cm^{-1} for the H_2−KCl and

H_2−NaCl isomers of C_{2v} symmetry (I). By contrast, the position shifts 11 cm^{-1} for the linear isomers involving close approach by the chloride ion (IV) but 12 cm^{-1} for the asymmetric forms, II. The calculated frequencies for the anion and asymmetrically bound H_2 both are equally consistent with the data for the isolated van der Waals adducts. The closest model to reality is that of $[NaAr_5][Cl(H_2)]$. Although frequencies were not obtained from theory, we have used a very good linear correlation between H−H distance and frequency to estimate 4101 cm^{-1} for the position of the H−H stretch. This is 16 cm^{-1} to the red of NaCl−H_2 (IV), but still short of the experimental result by about the same amount.

Summary

We set out to answer several questions from the matrix experiments that could not be resolved from experimental evidence alone. Does argon prevent the observation of cation-bound H_2 in matrices of MX and H_2? Yes, argon will displace hydrogen when the cation site is the preferred site of hydrogen coordination. Even in the absence of argon, H_2 preferentially binds at the fluoride side of KF. In explorations of the series of alkali metal chlorides from lithium to potassium the hydrogen appears to be in the process of being transferred to the anion. It is exclusively bound at the lithium and, in H_2−NaCl, there is minimal interaction between the chloride and H_2. The chloride of KCl is competitive for hydrogen coordination and presumably more so in RbCl and CsCl. With the exception of LiCl, the cation is never the sole site of coordination; rather binding involves some degree of anion binding. The inability of easy ortho−para transformations of H_2 may result in favorable associations of *o*-H_2 when the para form is not bound. This possibility could not be addressed in the matrix experiments.

We also asked if the complexity of the hydrogen spectrum in argon matrices of NaCl could be explained by differing interactions between the ion-pair and hydrogen. The analysis of this issue must be made in light of the simplicity of the spectrum for the other alkali metal halides. Of those systems explored, H_2−NaCl shows a substantial degree of cation influence. The presence of Ar can displace the hydrogen from the cation side, which should then yield an adduct that would be quite similar to the adducts of the other alkali metal chlorides. The radius ratio of Na^+ and Ar may be sufficiently large to allow some approach to the sodium by H_2 even when the coordination environment of the sodium is saturated with argon atoms. This opportunity may not be afforded by the smaller lithium ion in LiCl. Thus, NaCl is unique. Anion coordination is more likely for the heavier alkali metal halides and the size of lithium may not allow maximal coordination by argon and, at the same time, some degree of H_2 interaction.

Acknowledgment. We wish to thank J. S. Murray and P. A. Politzer for performing density functional calculations on NaCl and NaF to determine the nature of the electrostatic potential on the halide surface. Computer time was provided by the Alabama Supercomputer Network. M.L.M. would like to thank Sun Microsystems Computer Corp. for the award of an Academic Equipment Grant.

References and Notes

(1) E-mail: mckee@chem.auburn.edu.

(2) E-mail: rsweany@uno.edu.

(3) Ogden, J. S.; Sweany, R. L.; Rest, A. J. *J. Phys. Chem.* **1995**, *99*, 8485.

(4) Ogden, J. S.; Sweany, R. L. *Inorg. Chem.* **1997**, *36*, 2423.

(5) Bordiga, S.; Garrone, E.; Lamberti, C.; Zecchina, A.; Areán, C. O.; Kazansky, V. B.; Kustov, L. M. *J. Chem. Soc., Faraday Trans.* **1994**, *90*, 3367. Zecchina, A.; Areán, C. O. *Chem. Soc. Rev.* **1996**, 187. Larin, A. V. *Chem. Phys. Lett.* **1995**, *232*, 383; Moraldi, M.; Frommhold, L. *Phys. Rev. A* **1994**, *49*, 4508. Larin, A. V.; Cohen De Lara, E. *J. Chem. Phys.* **1994**, *101*, 8130. Cohen De Lara, E. *Mol. Phys.* **1989**, *66*, 479. Förster, H.; Frede, W. *Infrared Phys.* **1984**, *24*, 151. Larin, A. V.; Jousse, F.; Leherte, L.; Vercauteren, D. P. *Chem. Phys. Lett.* **1997**, *274*, 345. Kazansky, V. B.; Borovkov, V. Yu.; Karge, H. G. *J. Chem. Soc., Faraday Trans.* **1997**, *93*, 1843. Makarova, M. A.; Zholobenko, V. L.; Al-Ghefaili, K. M.; Thompson, N. E.; Dewing, J.; Dwyer, J. *J. Chem. Soc., Faraday Trans.* **1994**, *90*, 1047. Kustov, L. M.; Kazansky, V. B. *J. Chem. Soc., Faraday Trans.* **1991**, *87*, 2675. Bras, N. *J. Chem. Phys.* **1999**, *110*, 5943. Cohen de Lara, E. *Phys. Chem. Chem. Phys.* **1999**, *1*, 501. Kazansky, V. B. *J. Mol. Catal. A* **1999**, *141*, 83. Stéphanie-Victoire, F.; Cohen de Lara, E. *J. Chem. Phys.* **1998**, *109*, 6469.

(6) Dai, D. J.; Ewing, G. E. *J. Chem. Phys.* **1993**, *98*, 5050. Dai, D. J.; Ewing, G. E. *J. Chem. Phys.* **1994**, *100*, 8432. Heidber, J.; Dierkes, W.; Schönekäs, O.; Schwarte, R. *Ber. Bunsen-Ges. Phys. Chem.* **1994**, *98*, 131. Briquez, S.; Picaud, S.; Girardet, C.; Hoang, P. N. M.; Heidberg, J.; Vossberg, A. *J. Chem. Phys.* **1998**, *109*, 6435.

(7) Heinekey, D. M.; Oldham, W. J., Jr. *Chem. Rev.* **1993**, *93*, 913.

(8) Bender, B. R.; Kubas, G. J.; Jones, L. H.; Swanson, B. I.; Eckert, J.; Capps, K. B.; Hoff, C. D. *J. Am. Chem. Soc.* **1997**, *119*, 9179.

(9) Pitt, H. S.; Bär, M. R.; Ahlrichs, R.; Schnöckel, H. *Angew. Chem., Int. Ed. Engl.* **1991**, *30*, 832.

(10) Kirchner, N. J.; Bowers, M. T. *J. Chem. Phys.* **1987**, *86*, 1301.

(11) Sweany, R. L. Unpublished.

(12) Frisch, M. J.; Trucks, G. W.; Schlegel, H. B.; Scuseria, G. E.; Robb, M. A.; Cheeseman, J. R.; Zakrzewski, V. G.; Montgomery, J. A., Jr.; Stratmann, R. E.; Burant, J. C.; Dapprich, S.; Millam, J. M.; Daniels, A. D.; Kudin, K. N.; Strain, M. C.; Farkas, O.; Tomasi, J.; Barone, V.; Cossi, M.; Cammi, R.; Mennucci, B.; Pomelli, C.; Adamo, C.; Clifford, S.; Ochterski, J.; Petersson, G. A.; Ayala, P. Y.; Cui, Q.; Morokuma, K.; Malick, D. K.; Rabuck, A. D.; Raghavachari, K.; Foresman, J. B.; Cioslowski, J.; Ortiz, J. V.; Stefanov, B. B.; Liu, G.; Liashenko, A.; Piskorz, P.; Komaromi, I.; Gomperts, R.; Martin, R. L.; Fox, D. J.; Keith, T.; Al-Laham, M. A.; Peng, C. Y.; Nanayakkara, A.; Gonzalez, C.; Challacombe, M.; Gill, P. M. W.; Johnson, B.; Chen, W.; Wong, M. W.; Andres, J. L.; Gonzalez, C.; Head-Gordon, M.; Replogle, E. S.; Pople, J. A. *Gaussian 98*, Revision A.5; Gaussian, Inc.: Pittsburgh, PA, 1998.

(13) See the following references for need of full-core in MP2 calculations involving an alkali metal. (a) Hofmann, H.; Hänsele, E.; Clark, T. *J. Comput. Chem.* **1990**, *11*, 1147. (b) Partridge, H.; Bauschlicher, C. W.; Sodupe, M.; Langhoff, S. R. *J. Chem. Phys.* **1992**, *96*, 7871.

(14) Chałasiński, G.; Szczęśniak, M. M. *Chem. Rev.* **1994**, *94*, 1723.

(15) Jeziorski, B.; Moszynski, R.; Szalewicz, K. *Chem. Rev.* **1994**, *94*, 1887.

(16) Avoird, A. van der, Wormer, P. E. S.; Moszynski, R. *Chem. Rev.* **1994**, *94*, 1931.

(17) Thomas, J. R.; DeLeeuw, B. J.; Vacek, G.; Crawford, T. D. Yamaguchi, Y.; Schaefer, H. F. *J. Chem. Phys. 1993*, **99**, 403.

(18) Kaledin, A. L.; Heaven, M. C.; Bowman, J. M. *J. Chem. Phys.* **1999**, *110*, 10380.

(19) Fernández, B.; Koch, H. *J. Chem. Phys.* **1998**, *109*, 10255 and references therein.

(20) Soldán, P.; Lee, E. P. F.; Wright, T. G. *J. Chem. Soc., Faraday Trans.* **1998**, *94*, 3307.

(21) Mizoguchi, A.; Endo, Y.; Ohshima, Y. *J. Chem. Phys.* **1998**, *109*, 10539.

(22) Lenzer, T.; Yourshaw, I.; Furlanetto, M. R.; Reiser, G.; Neumark, D. M. *J. Chem. Phys.* **1999**, *110*, 9578.

(23) Stoicheff, B. P. *Can. J. Phys.* **1957**, *35*, 730.

(24) Murray, J. S.; Politzer, P. A. Unpublished data. Electrostatic potentials were obtained from structures which were optimized using a HF/6-311G basis set.

(25) Gough, K. M.; Yacowar, M. M.; Cleve, R. H.; Dwyer, J. R. *Can. J. Chem.* **1996**, *74*, 1139. Kołos, W.; Wolniewicz, *J. Chem. Phys.* **1967**, *46*, 1426.

(26) Charges calculated from dipole moment determinations cited by: Davis, S. L. *J. Chem. Phys.* **1988**, *88*, 1080. And M−X bond lengths cited by: Huheey, J. E.; Keiter, E. A.; Keiter, R. L. *Inorganic Chemistry*, 4th ed.; Harper Collins College Publishers: New York, 1993; pp A21-A33.

(27) Nichols, J. A.; Kendall, R. A.; Cole, S. J.; Simons, J. *J. Phys. Chem.* **1991**, *95*, 1074.

(28) Frenking, G.; Dapprich, S.; Köhler, K. F.; Koch, W.; Collins, J. R. *Mol. Phys.* **1996**, *89*, 1245.

(29) Miller, T. M.; Bederson, B. In *Advances in Atomic and Molecular Physics*; Bates, D. R., Bederson, B., Eds.; Academic Press: New York, 1977; Vol. 13, p 1f. Cited by: Frenking, G.; Koch, W.; Gauss, J.; Cremer, D. *J. Am. Chem. Soc.* **1988**, *110*, 8007.

(30) Kolos, W.; Wolniewicz, L. *J. Chem. Phys.* **1967**, *46*, 1426 and references therein.